AIP | APL Materials

Phase transition enhanced thermoelectric figure-of-merit in copper chalcogenides

David R. Brown, Tristan Day, Kasper A. Borup, Sebastian Christensen, Bo B. Iversen, and G. Jeffrey Snyder

Citation: APL Materials **1**, 052107 (2013); doi: 10.1063/1.4827595
View online: http://dx.doi.org/10.1063/1.4827595
View Table of Contents: http://scitation.aip.org/content/aip/journal/aplmater/1/5?ver=pdfcov
Published by the AIP Publishing

APL MATERIALS **1**, 052107 (2013)

Phase transition enhanced thermoelectric figure-of-merit in copper chalcogenides

David R. Brown,[1] Tristan Day,[1] Kasper A. Borup,[2] Sebastian Christensen,[2] Bo B. Iversen,[2] and G. Jeffrey Snyder[1,a]
[1]*Department of Applied Physics and Materials Science, California Institute of Technology, 1200 East California Boulevard, Pasadena, California 91125, USA*
[2]*Department of Chemistry and iNano, Aarhus University, Aarhus 8000, Denmark*

(Received 16 August 2013; accepted 17 October 2013; published online 14 November 2013)

While thermoelectric materials can be used for solid state cooling, waste heat recovery, and solar electricity generation, low values of the thermoelectric figure of merit, zT, have led to an efficiency too low for widespread use. Thermoelectric effects are characterized by the Seebeck coefficient or thermopower, which is related to the entropy associated with charge transport. For example, coupling spin entropy with the presence of charge carriers has enabled the enhancement of zT in cobalt oxides. We demonstrate that the coupling of a continuous phase transition to carrier transport in Cu_2Se over a broad (360–410 K) temperature range results in a dramatic peak in thermopower, an increase in phonon and electron scattering, and a corresponding doubling of zT (to 0.7 at 406 K), and a similar but larger increase over a wider temperature range in the zT of $Cu_{1.97}Ag_{.03}Se$ (almost 1.0 at 400 K). The use of structural entropy for enhanced thermopower could lead to new engineering approaches for thermoelectric materials with high zT and new green applications for thermoelectrics. [http://dx.doi.org/10.1063/1.4827595]

Thermoelectric generators are solid state heat engines. While a vapor compression heat engine, such as a steam engine, extracts useful energy from the cycle of a fluid's entropy change with temperature, a thermoelectric device utilizes an analogous cycle with a charged fluid (electrons in a solid semiconductor).[1] Thermoelectric conversion efficiency is determined by the thermoelectric figure of merit:

$$zT = \frac{\sigma \alpha^2 T}{\kappa}, \tag{1}$$

T is the absolute temperature, σ is the electrical conductivity, κ is the thermal conductivity, and α is the thermopower or Seebeck coefficient. Thermal conductivity is typically calculated from the thermal diffusivity D_T using the relation:

$$\kappa = \rho D_T c_p, \tag{2}$$

where ρ is the material density and c_p is the specific heat capacity. Unfortunately, existing materials are not efficient enough for the economical integration needed to make an impact on global energy consumption and the problem of climate change.[2] To address these problems, new strategies are needed to enhance thermoelectric efficiency. One such strategy is suggested by the recent work by Liu *et al.*[3] on the phase transition of Cu_2Se.

Thermopower is the electric potential produced by a temperature difference. Physically, thermopower is the ratio of entropy transported by moving charges to the charge transported.[4] In the

[a]jsnyder@caltech.edu

Kubo formalism, this can be divided into two terms:[5]

$$\alpha = -\frac{1}{k_b T}\frac{J_{qe}}{J_{ee}} - \frac{1}{e}\frac{\mu}{T}, \tag{3}$$

where k_b is Boltzmann's constant, T is temperature, e is the elementary charge, μ is chemical potential, and J_{qe} and J_{ee} are transport integrals representing heat transport per electron and current transported per electron.

Following Emin,[6] we refer to the first term as the "transport thermopower," $\alpha_{transport}$, and the second term as the presence thermopower, $\alpha_{presence}$. The transport thermopower represents the part of the thermopower that results from the manner in which charge is transported. It reflects contribution from the scattering interaction of the moving heat and charge, and the distortion transport effects on the state occupations and energies. The presence thermopower is the entropy change when a carrier is added to the system, irrespective of the means by which it was transported. Because it is a quasi-equilibrium term it can be expressed in a simple thermodynamic manner:[7]

$$\alpha_{presence} = \frac{-\mu}{eT} = \frac{1}{e}\left(\frac{\partial S}{\partial N}\right)_U, \tag{4}$$

where S is entropy, e is electron charge, N is number of carriers and U is internal energy. As the number of degrees of freedom coupled to carrier concentration increases, $\alpha_{presence}$ should increase as well. Typically, $\alpha_{presence}$ is dominated by the configurational entropy, derived by considering the different ways the charge carriers can occupy the available states.

By coupling the spin degree of freedom to entropy transport, increased thermopower in Na_xCoO_2 has been shown.[8,9] The differing spin degeneracy of electron-occupied and electron-unoccupied cobalt sites provides the mechanism for this coupling of carrier transport to entropy transport.[10] However, this strategy has thus far been limited to small changes in spin degrees of freedom of single ions; it remains an open question whether structures with more spin degrees of freedom can be coupled to charge transport.

Here we consider coupling the carrier transport to degrees of freedom associated with the structural changes of a phase transition. A phase transition is always associated with an entropy change because there is always a concurrent transformation in system symmetries.[11] In continuous (i.e., second order) phase transitions the entropy will change over an extended temperature range. Typically these transformations show critical power law dependence of thermodynamic parameters such as entropy and heat capacity below the phase transition. For example:

$$S \propto \left(\frac{Tc - T}{Tc}\right)^r, \tag{5}$$

where T_c is the critical temperature of the phase transition, and r is the critical exponent.

Copper (I) selenide is a p-type semiconductor,[12] that above 410 K Cu_2Se becomes super-ionic, which is characterized by its disordered Cu^+ ions, and shows good thermoelectric properties.[13] Except at the highest temperatures, charge transport is dominated by holes rather than Cu^+ ions. As the temperature drops below 410 K, the ion mobility decreases[14] and eventually the Cu ions become ordered.[15] It is known that copper (I) selenide can be copper deficient ($Cu_{2-\delta}Se$) with copper vacancies, and this has a large effect on transport properties and the phase structure.[16] Horvatic and Vucic showed that the ion conductivity of $Cu_{1.99}Se$ increases from 1 S/m at 374 K to almost 100 S/m at 410 K,[14] demonstrating it to have a super-ionic phase transition. Below 374 K and above 410 K, he found that the ion conductivity followed an Arrhenius law with $E_A = 0.29$ eV and $E_A = 0.07$ eV, respectively. Each of these temperatures had been previously identified as corresponding to a phase transition in $Cu_{2-\delta}Se$ ($\delta < 0.045$).[16,17] In the intermediate temperature range, the ion conductivity changed rapidly. This behavior is indicative of a continuous phase transition in a super-ionic material.[18,19]

An observation of not only structural entropy change at the phase transition but also of structural entropy transport is given by Korzhuev and Laptev;[20] they measured a sharp peak in the thermodiffusion of Cu^0 in Cu_2Se at the 410 K phase transition. From this they calculated a heat of transport

of Cu atoms of 1 eV. Conservation of particles requires that

$$Q^*_{Cu^0} = Q^*_{Cu^+} - Q^*_p = qT(\alpha_{Cu^+} - \alpha_p), \tag{6}$$

where $Q^*_{Cu^0} = 1$ eV corresponds to $\alpha_{Cu^+} - \alpha_p = 2500\ \mu$V/K, implying a very large value for α_{Cu^+} at the phase transition.

If the structural entropy change of a continuous phase transition could be coupled to carrier transport, a substantial enhancement in thermopower may be obtainable. The number of degrees of freedom associated with a structural transformation scales as the number of atoms in the system rather than the number of carriers. For a typical thermoelectric material with a carrier concentration of 10^{20} cm^{-3}, there are 100 times as many atoms as there are charge carriers. Thus, the potential thermopower enhancement by this mechanism may be much larger than that from coupling the spin degree of freedom.[8] Here, we report observing a greater than 100% increase in the zT of Cu_2Se, to a maximum of 0.7 at 406 K, concurrent with a continuous phase transition and driven by a 55% increase in thermopower. Temperature-resolved powder X-ray diffraction (PXRD) analysis reveals a concurrent continuous change in the material's structure (Fig. 1 and Fig. S1 of the supplementary material[21]). $Cu_{1.97}Ag_{.03}Se$ shows a 150% increase in zT to a maximum of 1.0 at 400 K.

For the purpose of discussion, when we refer to Cu_2Se or copper selenide we mean it to be applicable to $Cu_{2-\delta}Se$ with any observed δ that shows the same low temperature structure and is a distinct phase from $Cu_{1.8}Se$. The related material, $Cu_{1.97}Ag_{.03}Se$ was extensively studied as a high temperature thermoelectric by NASA-JPL (National Aeronautics and Space Administration-Jet Propulsion Laboratory) in the 1970s, but had issues in device implementation due to the electromigration of Cu^+ ions.[22] Below the phase transition, the ion conductivity is two to three orders of magnitudes lower,[23] so that problem would be strongly mitigated in the temperature range addressed in this manuscript.

The thermopower of Cu_2Se shows a dramatic increase above 360 K with a peak at 403 K (Fig. 2(a)). The onset of linear behavior at 410 K indicates the phase transition is complete above this temperature. The thermopower below this temperature is remarkably stable, indicating it is a steady state property of the material. The sample was held at an average temperature of 390 K and a temperature difference of 16 K for 13 h. The measured thermopower, 152 μV/K, is varied by less than 1% during this time period.

PXRD scans were performed both above and below the phase transition temperature. The high temperature phase is similar to the tetrahedral-coordinated antifluorite structure (space group $Fm\bar{3}m$) but with copper additionally occupying interstitials on the octahedral and trigonal planar sites.[24] This model describes the diffraction data well, however, some disagreement between intensities still exists. Incorporation of additional interstitials resulted in unstable refinements, and the disagreement is instead believed to be due to the dynamic movement of copper and resulting smearing of the electron density.[24,25] While the high temperature structure is relatively simple, the low temperature structure is not thoroughly understood. Kashida and Akai[15] proposed a monoclinic unit cell ($a = c = 7.14$ Å, $b = 81.9$ Å, $\beta = 120^\circ$) with ordering of copper vacancies, while Vučić *et al.* proposed an even larger monoclinic cell ($a = c = 12.30$ Å, $b = 40.74$ Å, $\beta = 120 \pm 1^\circ$).[16] Neither of these unit cells were able to describe the position of all reflections at low angles, indicating the structure to be even more complicated. Therefore, no structural refinement below the phase transition is possible from PXRD at present, and the order parameter is not easily obtained from this method.

Nevertheless, temperature resolved PXRD data confirm a continuous transformation of the atomic structure (Fig. 2(b)), which will be closely related to the order parameter. Fast PXRD scans (2θ range 23°–46°) were performed from room temperature to 420 K while heating at 1 K/min, resulting in diffractograms with 3–4 K spacing. The peak intensities and positions were extracted and observed to change smothly until the phase transition temperature is reached, at which point only the the high temperature antifluorite peaks remain. Upon cooling, the high temperature reflections transform smoothly into peaks belonging to the low temperature phase. No other refelctions are withing the scanned 2θ range. Using the temperature dependence of the position of these reflection, an estimate of

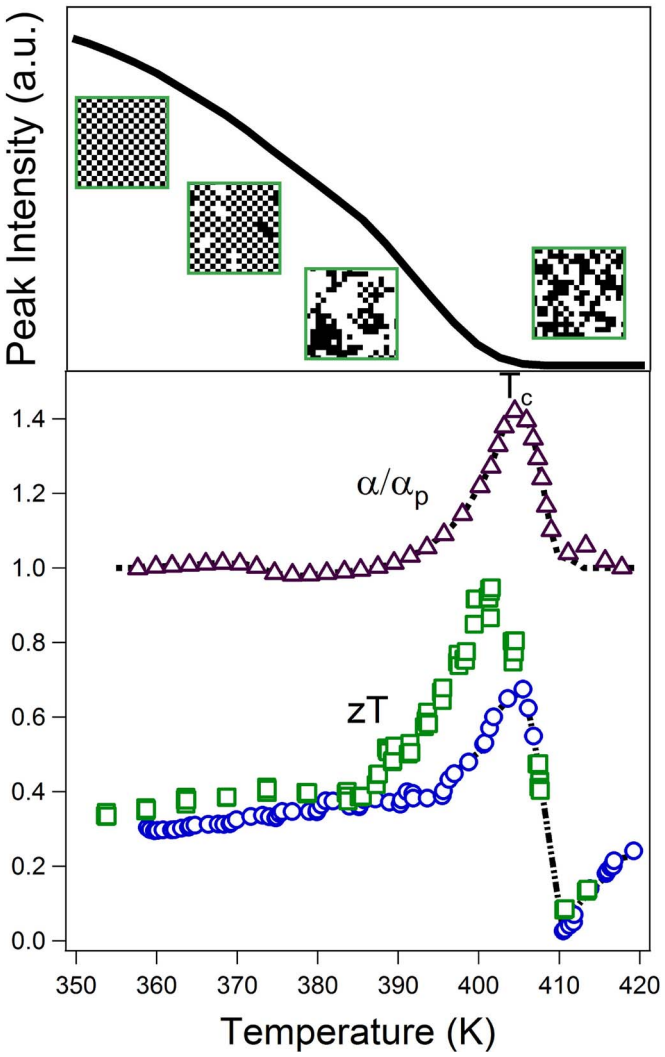

FIG. 1. Dramatic increase in thermoelectric efficiency near the phase transition in Cu_2Se (blue circles) and $Cu_{1.97}Ag_{.03}Se$ (green squares). In a continuous phase transition, peaks that break the symmetry of the higher temperature phase (top) decrease smoothly to zero at the critical temperature T_C. The integrated intensity corrected for the background intensity of the Cu_2Se PXRD peak located at 26° in Figure 2(b) is plotted here. In this transition region, fluctuations lead to correlations at a critical length scale, which changes with temperature, and also to an increase in entropy. This ordering and fluctuations are represented by the inset images. Near the phase transition fluctuations occur at all length scales. The thermoelectric figure of merit, zT (bottom), doubles in the critical region below the phase transition at 410 K. The doubling in zT above 390 K in Cu_2Se is primarily due to the increase in measured thermopower (α) compared to that expected from a rigid band model[1] (α_p) and the measured Hall carrier concentration.

the molar volume can be extracted during the phase transition even without knowledge of the structure (Fig. 3(a)).

A pair distribution function (p.d.f.) was obtained from total scattering data. It describes the distribution of distances between pairs of atoms in the structure (Figs. 3(b) and 3(c)). Even without modeling the data it is possible to extract qualitative information. By studying the high-temperature structure of Cu_2Se it is clear that the peak at 4.1 Å, Fig. 3(b), is a superposition of the shortest Cu–Cu and Se–Se distances in the [110]-direction (cubic nomenclature). Above 300 K the peak becomes increasingly asymmetric, indicative of multiple Cu–Cu distances in the high-temperature phase related to the disorder of Cu interstitials. At low temperature the Cu orders to form a superstructure. The superstructure formation is most clearly seen in the region 8 Å–9.5 Å, Fig. 3(c). This range corresponds to Cu–Cu distances in the [110]-direction in adjacent cubic unit cells. Below 410 K

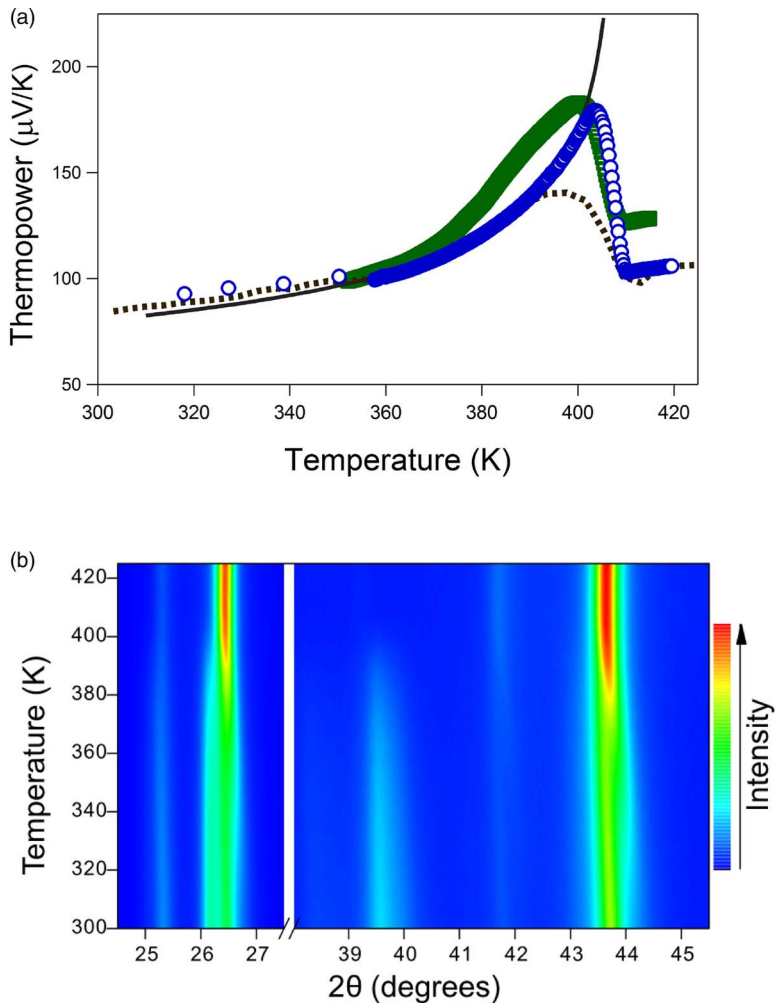

FIG. 2. (a) Thermopower (α) peak in Cu_2Se (blue circles) and $Cu_{1.97}Ag_{.03}Se$ (green squres). The increase in thermopower, shown with a critical exponent fit, is clearly associated with the continuous phase transition. Between 390 K and 410 K, there is a significant increase in the measured thermopower above that predicted by the change in Hall carrier concentration (dotted line). In this region, the entropy of the phase transition (Figure 4(c)) also increases the thermopower. (b) Continuous transformation of the PXRD spectrum of Cu_2Se on slow heating (1 K/min). The continuous disappearance and transformations of peaks are indicative of a 2nd order transformation of the structure. The same is observed under slow cooling (not shown), indicating that the gradual transformation is not due to kinetic limitations.

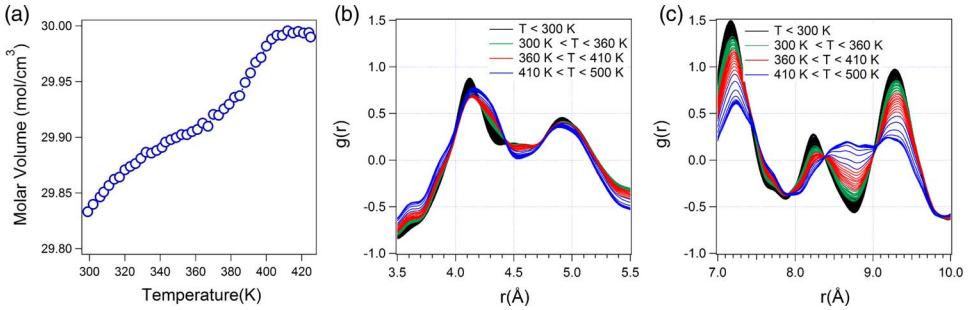

FIG. 3. (a) Molar volume through the phase transition from the [111] reflection of the high temperature phase. The molar volume is continuous through the phase transition, indicative of a second order phase transition. [(b) and (c)] Reduced p.d.f., g(r) from synchotron total scattering. Upon increase in temperature a number of additional peaks emerge in the p.d.f. indicating the disordering of Cu on interstitial sites.

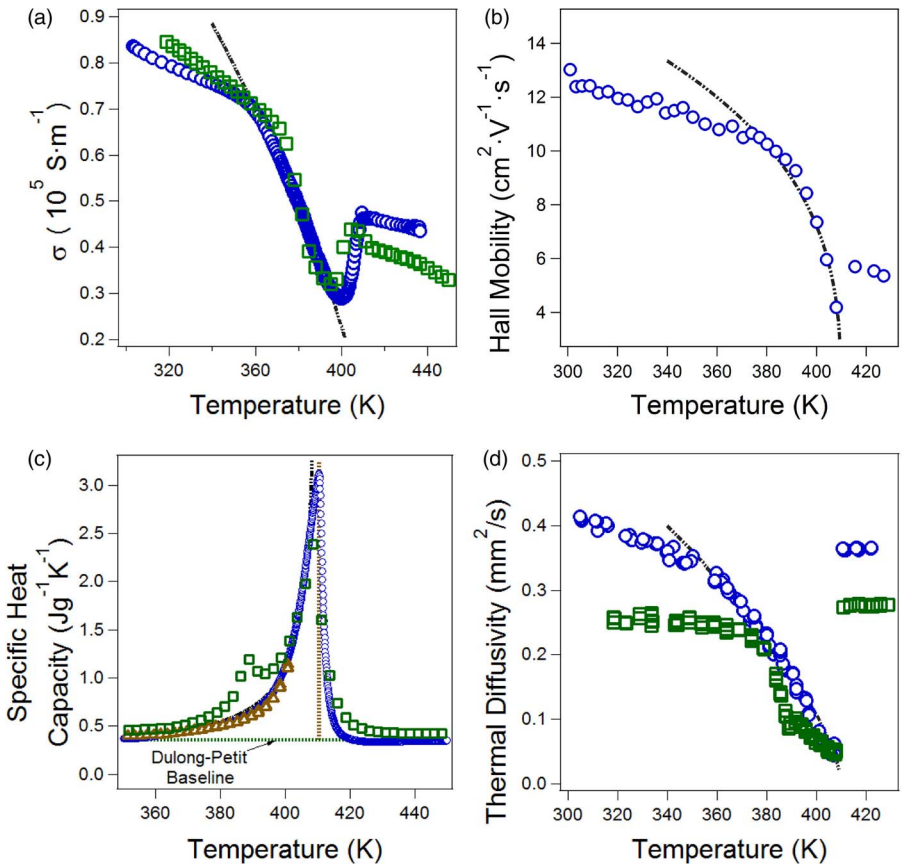

FIG. 4. The physical properties of Cu_2Se (blue circles) and $Cu_{1.97}Ag_{.03}Se$ (green squares) show behavior strongly atypical of most good thermoelectrics near the phase transition temperature. Black dashed lines represent a critical fit with $T_c = 410$ K for the Cu2Se data. D_T and μ_H, which directly depend on phonon and electron scattering, show particularly good agreement with critical exponent analysis. (a) Electrical conductivity (σ) versus temperature (T). The data suggest phase transitions at 360 K and 410 K. Critical exponent is $r = 0.70$. (b) Hall mobility (μ_H) versus temperature (T). Between 360 K and 410 K the data fit well to a critical power law. Critical exponent is $r = 0.32$. The Hall coefficient of Cu1.97Ag.03Se is discussed in Figure 6(b).(c) Specific heat capacity versus temperature (T). Measured by DSC on heating at 5 K/min, (blue circles) and by PPMS on Cu_2Se (brown triangles). Cu_2Se data show a clear lambda shape, indicating a continuous increase in entropy, with a peak at 410 K. The data exceed the Dulong–Petit values (green line) in the phase transition region. Critical exponent is $r = -0.68$. (d) Thermal diffusivity (D_T) versus temperature (T). Between 360 K and 410 K the data fit well to a critical power law. Critical exponent is r = 0.80.

there are two distinct peaks at 8.2 Å and 9.3 Å. However; in the high temperature phase the same region is a continuum of overlapping peaks arising from the disorder of Cu. The changes of the p.d.f. are gradual indicating that the ordering of Cu-interstitials occurs over a wide temperature range.

At temperatures less than 360 K and above 410 K, the Hall carrier concentration, n_H, is temperature-independent. Between 360 K and 410 K, the Hall carrier concentration dips until it reaches a minimum of 2.7×10^{20} cm^{-3} (Fig. S2b of the supplementary material[21]). This minimum occurs at 393 K, 10 K lower than the maximum and minimum in thermopower and electrical conductivity, respectively. The conductivity data below 360 K follow the linear power law identified by Vucic *et al.*,[26] indicating a second order transition at 360 K. We therefore consider 360–410 K to be the phase change region. Below and above this range the Cu_2Se sample is clearly in its stable low temperature phase and high temperature phase, respectively.

Below 355 K and above 425 K the heat capacity (Fig. 4(c)) gives a baseline value of 0.374 J g^{-1} K^{-1}, consistent with the Dulong–Petit c_p for Cu_2Se, 0.361 J g^{-1} K^{-1}. The 60 K breadth

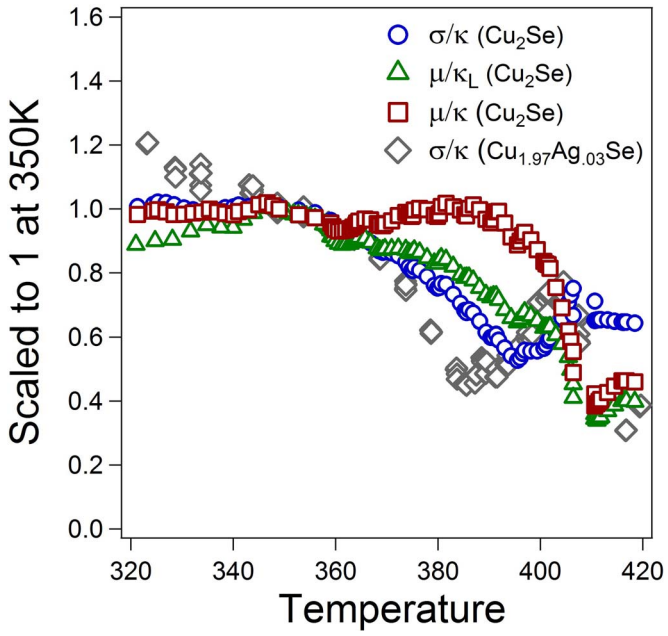

FIG. 5. Ratio of electrical transport variables to thermal transport variables (scaled to 1 at 350 K). Though thermal conductivity decreases between 360 K and 410 K, this decrease is more than counteracted by a decrease in electrical mobility over the same range. The observed increase in zT is not due to the reduction of the thermal conductivity via preferential scattering of phonons over electrons.

of the peak is indicative of the continuous nature of the transition. In the transition region there is a lambda-type peak, as is characteristic of continuous phase transitions in ionic conductors.[19]

Both thermopower (Fig. 2(a)) and electrical conductivity (Fig. 4(a)) show near-critical type behavior, while both thermal diffusivity (Fig. 4(d)) and Hall mobility (Fig. 4(b)) show clear fits to critical power laws (Eq. (5)). As both thermal diffusivity and Hall mobility are scattering-dominated phenomena, their adherence to a power law is strong evidence that the principal scattering mechanism is a result of the continuous phase transition.

By applying Eqs. (1) and (2) to the transport data described above and a measured density of 6.7 g cm^{-3}, we were able to determine zT (Fig. 1). zT shows a peak value of 0.7 at 406 K, which is over twice the zT determined at a temperature 20 K lower. This near doubling in zT near the phase transition is driven by a corresponding 55% enhancement in thermopower. Because there is a continuous phase transition occurring while the zT is peaking, a new mechanism for high zT, associating the transport properties with the critical phenomena of the phase transition is necessary to explain the data.

Similarly, we were able to determine zT for $Cu_{1.97}Ag_{.03}Se$ to peak at 1.0 at 400 K, which is two and a half times the zT at a temperature 20 K lower. This peak is uniformly larger and broader than that of Cu_2Se (Fig. 1), which is driven by a broadening of the thermopower peak (Fig. 2) and an improvement in the ratio of σ to κ (Fig. 5) Hall measurements have been thus far unable to resolve the carrier concentration of the measurements. As a recent publication confirms,[27] Ag substituted Cu_2Se shows an n-type Hall coefficient in its low temperature phase despite having a p-type Seebeck. As Hall coefficient is weighted quadratically by the mobility of different carriers, an n-type band associated with the Ag substitution may explain this effect. PXRD data (Fig. 6(a)) shows there to be CuAgSe type impurities. Thermal diffusivity (Fig. 4(c)) and heat capacity (Fig. 4(d)) show two extrema at 388 K and 406 K. In the intermediate region the Hall coefficient steadily changes sign (Fig. 6(b)). This suggests that the interaction of the Ag with the majority phase extends the phase transition region significantly.

The decrease in μ_H, σ, and thermal conductivity (κ) (Figure S2a of the supplementary material[21]) indicate that scattering of phonons and electrons is substantially increased near the phase transition.

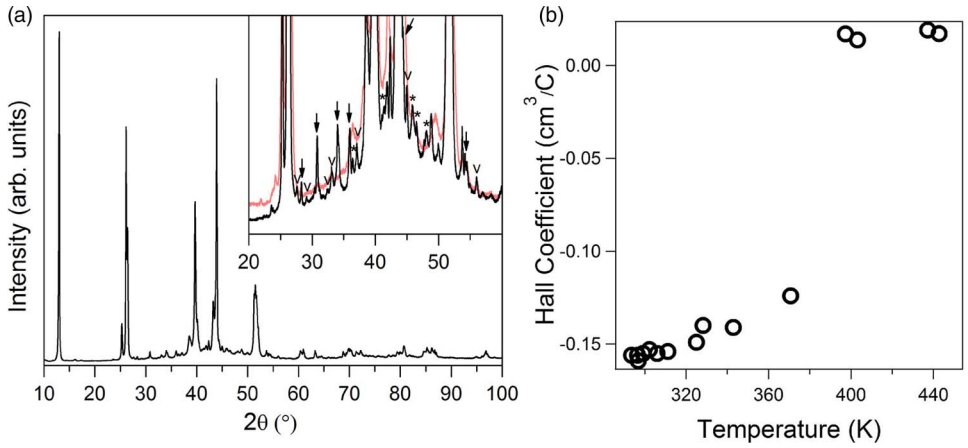

FIG. 6. (a) Room temperature PXRD of a $Cu_{1.97}Ag_{0.03}Se$ pellet. The insert shows the same pattern (black) with a vertical scale that better shows the secondary phases. A room temperature pattern of Cu_2Se is shown in transparent red for reference. Peaks identified as CuAgSe are marked with arrows, impurity peaks still present at high temperature with asterisks, and peaks which disappear at the phase transition but do not correspond to a Cu_2Se peak are marked with v's. These peaks are believed to belong to one or more impurities, which dissolve. (b) Hall coefficient of $Cu_{1.97}Ag_{0.03}Se$. Negative Hall coefficient is observed in the low temperature phase. As the high temperature phase is approached, the Hall coefficient becomes positive. This likely indicates an interaction between the Ag impurities and the main phase of Cu_2Se.

However, this scattering is not directly responsible for the zT increase as indicated by the decreasing ratio of μ_H and σ to thermal conductivity (κ) and lattice thermal conductivity (κ_L) (Fig. 5). κ_L was calculated assuming a single parabolic band (SPB) and acoustic phonon scattering.

In the degenerate limit of the SPB, the thermopower can be expressed as

$$\alpha_p = \frac{\pi^{8/3} k_b^2}{3eh^2} n_H{}^{-2/3} T m^* (1+\lambda), \tag{7}$$

in which n_h is the Hall carrier concentration, m^* is the effective mass. The scattering parameter, denoted here by λ, describes the energy dependence of the electron scattering; for the typical mechanism of acoustic phonon scattering, $\lambda = 0$. From room temperature to 388 K, the thermopower can be completely explained by Eq. (7) with a constant m^* and λ. From 389 K to 410 K, the measured data exceed the degenerate band prediction, with the temperature range and size of the zT peak explained by the additional thermopower (Figure 1). This gradual divergence in the thermopower indicates that the continuous phase transition is enhancing the thermopower.

Unusual transport effects previously have been observed near the critical temperature in Cu_2Se..[12,28] Liu *et al.* reports a zT peak[3] by assuming none of the heat released as measured by Differential Scanning Calorimetry (DSC) is associated with the Seebeck peak. Instead Liu *et al.* calculate κ (from Eq. (2)) and zT using only the Dulong-Petit heat capacity ($C_p = 3k_b$/atom) which assumes the DSC peak is due to the enthalpy of a first order structural transformation. The Physical Property Measurement System (PPMS) heat capacity data in this work, however, indicates that the measured DSC enthalpy is a steady-state property of the material (Fig. 3(c)), and therefore here DSC heat capacity is used to calculate κ and zT. This analysis is elaborated on in the supplementary materials, section IV.[21]

We suggest that a great portion of the thermopower increase in Cu_2Se might be explained by the coupling of structural degrees of freedom associated with the phase transition to carrier transport. In the Ginzburg–Landau picture, the portion of the free energy corresponding to the phase change behavior can be expressed as a function of two variables, temperature (T) and the order parameter m. Following Eq. (4), the phase-entropy portion of the electronic thermopower can be written as

$$\alpha_{Phase-Entropy} = \frac{1}{e}\frac{\partial S}{\partial m}\left(\frac{\partial m}{\partial N_p}\right)_U. \tag{8}$$

If the fundamental ordering process depends upon the carrier concentration, $\left(\frac{\partial m}{\partial N_p}\right)_U$ will be large, and the thermopower will be enhanced. In $Cu_{2-\delta}Se$ the order parameter must vary with the local Cu^+ concentration as the transition temperature changes with δ.[16] Korzhuev and Laptev's[20] thermodiffusion experiment found that $Q^*_{Cu^0}\left(\approx T\frac{\partial S_{Cu}}{\partial N_{Cu}}\right)$ increases to a maximum of $\frac{1}{e}\frac{\partial S_{Cu}}{\partial N_{Cu}} \approx 2500\,\mu$V/K at the phase transition temperature. In the supplementary material,[21] we show that this enhancement in the Cu^0 entropy of transport is consistent with the ion conductivity data measured by Horvatic *et al.*[14] If the ion conductivity increase is due to increasing occupation of higher energy interstitials, a $\frac{1}{e}\frac{\partial S_{Cu}}{\partial N_{Cu}}$ of order $10^3\,\mu$V/K can be obtained.[14] This increased occupation is consistent with our p.d.f. analysis above, other literature analysis,[24,25] and understanding of super-ionic phase transitions.[18]

Critically increased entropy may be present in other materials systems. Reports on Ag_2Se[29] and $AgCrSe_2$,[30] which are also ion transporting materials, indicate a small thermopower enhancement near a phase transition, though there is no evidence that this is associated with critical phenomena. The temperature of the continuous transition in the CuI–AgI system shows a composition dependence.[31] The effect on thermopower from phase entropy is likely not limited to mixed ion-electron conductors. Any material in which the entropy associated with a phase transition might be coupled to transport is a candidate. For example, the magnetic ordering phase transition associated with giant magnetoresistance is often accompanied by a corresponding significant thermopower change.[32] Applying a magnetic field to these materials induces ordering and results in a corresponding reduction in thermopower.

In order to understand and engineer this phenomenon, substantial future work needs to be done. The ionic properties, both the conductivity[20] and the thermopower,[33] may need to be measured and considered when engineering these materials. Further synchotron and neutron crystallographic work may be able to uncover the structure and order parameter. The best thermoelectric performing materials in this class of compound are yet to be synthesized. Because the enhancement of the thermopower closely follows the observed increase in zT, this work strongly indicates a new mechanism for enhanced thermoelectric performance: the coupling of structural entropy to transport through the thermodynamics of the phase transition. Ag substitution of Cu_2Se has shown an even broader and larger enhancement in zT, suggesting a specific path forward for developing this new class of materials.

The authors would like to acknowledge Huili Liu, Dr. Xun Shi and Dr. Lidong Chen of SICCAS for discussions and assistance with heat capacity measurements; Alex Z. Williams and the NASA-JPL for aid in measuring the Hall coefficient; and Resnick Institute and Air Force Office of Science Research for support. Use of the Advanced Photon Source was supported by the U. S. Department of Energy, Office of Science, Office of Basic Energy Sciences, under Contract No. DE-AC02-06CH11357.

[1] G. J. Snyder and E. S. Toberer, Nature Mater. **7**(2), 105 (2008).
[2] L. E. Bell, Science **321**(5895), 1457 (2008).
[3] H. Liu, X. Shi, M. Kirkham, H. Wang, Q. Li, C. Uher, W. Zhang, and L. Chen, Mater. Lett. **93**, 121 (2013).
[4] C. Goupil, W. Seifert, K. Zabrocki, E. Muller, and G. J. Snyder, Entropy **13**(8), 1481 (2011).
[5] R. Kubo, M. Yokota, and S. Nakajima, J. Phys. Soc. Jpn. **12**(11), 1203 (1957).
[6] D. Emin, Phys. Rev. B **59**(9), 6205 (1999).
[7] A. L. Rockwood, Phys. Rev. A **30**(5), 2843 (1984); P. M. Chaikin and G. Beni, Phys. Rev. B **13**(2), 647 (1976).
[8] Y. Y. Wang, N. S. Rogado, R. J. Cava, and N. P. Ong, Nature (London) **423**(6938), 425 (2003).
[9] W. Koshibae, K. Tsutsui, and S. Maekawa, Phys. Rev. B **62**(11), 6869 (2000); S. Mukerjee and J. E. Moore, Appl. Phys. Lett. **90**(11), 112107 (2007).
[10] S. Mukerjee, Phys. Rev. B **72**(19), 195109 (2005).
[11] C. N. R. Rao and K. J. Rao, *Phase Transitions in Solids : An Approach to the Study of the Chemistry and Physics of Solids* (McGraw-Hill, New York, 1978).
[12] F. Elakkad, B. Mansour, and T. Hendeya, Mater. Res. Bull. **16**(5), 535 (1981).
[13] H. Liu, X. Shi, F. Xu, L. Zhang, W. Zhang, L. Chen, Q. Li, C. Uher, T. Day, and G. J. Snyder, Nature Mater. **11**(5), 422 (2012).
[14] M. Horvatic and Z. Vucic, Solid State Ionics **13**(2), 117 (1984).
[15] S. Kashida and J. Akai, J. Phys. C **21**(31), 5329 (1988).
[16] Z. Vučić, O. Milat, V. Horvatić, and Z. Ogorelec, Phys. Rev. B **24**(9), 5398 (1981).

[17] N. N. Sirota, M. A. Korzhuev, M. A. Lobzov, N. K. Abrikosov, and V. F. Bankina, Dokl. Akad. Nauk SSSR **281**(1), 75 (1985).
[18] J. B. Boyce and B. A. Huberman, Phys. Rep. **51**(4), 189 (1979).
[19] F. L. Lederman, M. B. Salamon, and H. Peisl, Solid State Commun. **19**(2), 147 (1976).
[20] M. A. Korzhuev and A. V. Laptev, Fiz. Tverd. Tela (Leningrad) **29**(9), 2646 (1987).
[21] See supplementary material at http://dx.doi.org/10.1063/1.4827595 for thermoelectric Cu_2Se.
[22] D. R. Brown, T. Day, T. Caillat, and G. J. Snyder, J. Electron. Mater. **42**(7), 2014 (2013).
[23] V. A. Chatov, T. P. Iorga, and P. N. Inglizyan, Sov. Phys. Semicond **14**(4), 474 (1980).
[24] K. Yamamoto and S. Kashida, Solid State Ionics **48**(3-4), 241 (1991).
[25] S. A. Danilkin, M. Avdeev, T. Sakuma, R. Macquart, C. D. Ling, M. Rusina, and Z. Izaola, Ionics **17**(1), 75 (2011).
[26] Z. Vucic, V. Horvatic, and Z. Ogorelec, J. Phys. C **15**(16), 3539 (1982).
[27] S. Ballikaya, H. Chi, J. R. Salvador, and C. Uher, J. Mater. Chem. A **1**(40), 12478 (2013).
[28] Z. Ogorelec and B. Celustka, J. Phys. Chem. Solids **27**(3), 615 (1966); K. Okamoto, Jpn. J. Appl. Phys. **10**(4), 508 (1971); X. X. Xiao, W. J. Xie, X. F. Tang, and Q. J. Zhang, Chin. Phys. B **20**(8), 087201 (2011); G. Bush and P. Junod, Helv. Phys. Acta **32**, 567 (1959).
[29] C. Xiao, J. Xu, K. Li, J. Feng, J. Yang, and Y. Xie, J. Am. Chem. Soc. **134**(9), 4287 (2012).
[30] F. Gascoin and A. Maignan, Chem. Mater. **23**(10), 2510 (2011).
[31] M. Kusakabe, Y. Ito, and S. Tamaki, J. Phys. Condens. Matter **8**(37), 6851 (1996).
[32] M. Jaime, M. B. Salamon, K. Pettit, M. Rubinstein, R. E. Treece, J. S. Horwitz, and D. B. Chrisey, Appl. Phys. Lett. **68**(11), 1576 (1996); C. J. Liu, C. S. Sheu, T. W. Wu, L. C. Huang, F. H. Hsu, H. D. Yang, G. V. M. Williams, and C. J. C. Liu, Phys. Rev. B **71**(1), 014502 (2005).
[33] M. K. Balapanov, I. B. Zinnurov, and G. R. Akmanova, Phys. Solid State **48**(10), 1868 (2006).